Available online at www.sciencedirect.com

Journal of the European Ceramic Society 29 (2009) 1729–1733

www.elsevier.com/locate/jeurceramsoc

Effect of MnO_2 on the dielectric and piezoelectric properties of alkaline niobate based lead free piezoelectric ceramics

Henry Ekene Mgbemere, Ralf-Peter Herber, Gerold A. Schneider*

Institute of Advanced Ceramics, Hamburg University of Technology,
Denickestrasse 15, 21073, Hamburg, Germany

Received 30 July 2008; received in revised form 17 October 2008; accepted 23 October 2008
Available online 10 December 2008

Abstract

Lead free ferroelectric ceramics of the KNN–$LiTaO_3$–$LiSbO_3$ system were prepared using the mixed oxide route. This work reports the effect of doping $(K_{0.44}Na_{0.52}Li_{0.04})(Nb_{0.86}Ta_{0.1}Sb_{0.04})O_3$ produced through the conventional solid state sintering method with different amounts of MnO_2. With 1 mol% of the dopant, ~96.5% of the theoretical density of the ceramics was achieved while grain growth inhibition was attained through pinning of the grain boundary movement. A polymorphic phase transition (PPT) was induced in the ceramic from the orthorhombic crystal structure to the tetragonal structure with increasing dopant amount. At lower temperatures, the doped samples had higher epsilon values but there was a decrease in both T_c (from 333 °C to 249 °C) and epsilon value at T_c (from ≈9500 to <6000). At temperatures below 300 °C however, the loss tangent in the doped samples (≈2.5 mol%) was much lower and steady when compared to the undoped one. The ferroelectric properties were slightly lowered with the addition of MnO_2. The remnant polarisation (P_r) was lowered from ~18 μC/cm² to ~9 μC/cm², the coercive field (E_c) from ~8.5 kV/cm to ~6.2 kV/cm and the piezoelectric charge coefficient (d_{33}) decreased as well.

Keywords: Dielectric properties; Ferroelectric properties; Piezoelectric properties; Perovskites; Lead free

1. Introduction

Lead zirconate titanate (PZT) based piezoceramics have been widely used in the manufacture of actuators, sensors, transducers and in other electromechanical devices because of their excellent piezoelectric properties. However lead in most cases constitutes at least 60% of the composition of these piezoceramics. Lead as an element is highly toxic and because of its volatility and high vapour pressure, is released to the atmosphere during sintering causing serious environmental and health problems. Another cause for concern is its disposal at the end of the life cycle of these products.

Considering all these health concerns posed by lead, multinational governments like the European Union have enacted laws that ban the use of lead in the manufacture of many products.[1] In the field of electro-ceramics, concessions were allowed considering the fact that many of the lead free ferroelectric ceramics have piezoelectric properties that are inferior when compared to those of lead based piezoceramics.

Lead free piezoceramics are classified into categories based on their crystal structure. The bismuth layered type (e.g. $Bi_4Ti_3O_{12}$)), the tungsten bronze type (e.g. $BaNaNb_5O_{15}$) and perovskite structures (e.g. KNN) are the most important ones. A lot of research has been carried out on lead free piezoceramics in the last 50 years but in the last 7 years, the momentum has tremendously increased accounting for more than 75% of all published works. $KNbO_3$,[2] (Ba,Sr)TiO_3 (BST), $Bi_{0.5}K_{0.5}TiO_3$[3] (BKT), $(Bi_{0.5}Na_{0.5})TiO_3$[4] (BNT) and (K,Na)NbO_3[5] based ceramics have been well investigated. Among these materials, $K_xNa_{1-x}NbO_3$ (KNN) which is a solid solution of ferroelectric $KNbO_3$ and antiferroelectric $NaNbO_3$ appears to be the most promising because of its comparably higher piezoelectric properties, large electromechanical coupling coefficients and high Curie temperature (≈420 °C).[6]

However the sinterability of this KNN ceramics has been difficult without the use of special techniques like hot pressing because of the high volatility of the alkaline element components

---

* Corresponding author.
E-mail addresses: henrymgbemere@yahoo.com (H.E. Mgbemere), g.schneider@tu-harburg.de (G.A. Schneider).

0955-2219/$ – see front matter © 2008 Elsevier Ltd. All rights reserved.
doi:10.1016/j.jeurceramsoc.2008.10.012

Table 1
Data showing the density, dielectric and piezoelectric properties of KNN–$LiTaO_3$–$LiSbO_3$ with different amounts of MnO_2 at room temperature.

Composition	0 mol%	0.5 mol%	1 mol%	2.5 mol%
Theoretical density (g/cm^3)	4.79	4.8	4.81	4.83
Relative density (%)	94.3	95.7	96.4	94.4
Coercive field (E_c) (kV/mm)	8.6	5.6	5.8	6.2
Remanent polarisation (P_r) (μC/cm^2)	18.3	8.6	8.3	8.9
Relative permittivity (ε_r) @ 1 kHz	1305	1440	1528	1680
Tan δ @ 1 kHz	0.146	0.028	0.018	0.026
Piezoelectric constant (d_{33}) (pm/V) (small signal)	220	171	171	176
Piezoelectric constant (d_{33})[a] (pm/V) (large signal)	362.9	261.5	331.4	209.1

[a] The d_{33} values from large signal measurements were obtained from the slope of the uniaxial strain hysteresis graphs.

at high temperature. There is a degradation of the properties ($d_{33} = 80$ pC/N, $K_p = 0.36$, $\rho = 4.25$ g/cm^3)[5] when they are sintered in air whereas hot pressing leads to better properties ($d_{33} = 160$ pC/N, $K_p = 0.45$, $\rho = 4.46$ g/cm^3).[6]

To improve the sinterability and piezoelectric properties of KNN ceramics, a lot of different additives either as elements or compounds and synthesis techniques have been used. Some of these include: KNN–Ba,[7] KNN–$SrTiO_3$,[8,9] KNN–$LiNbO_3$,[10] KNN–$LiTaO_3$,[11] KNN–$LiSbO_3$,[12] (K,Na,Li)(Nb,Ta,Sb)O_3[13] and pure KNN with sintering aids like CuO,[14] ZnO,[15] MnO_2[16] and Bi_2O_3.[17]

The KNN–$LiTaO_3$–$LiSbO_3$ composition which was first reported by Saito et al.[13] remains one of the best so far in terms of piezoelectric properties. The electronegativity of Sb^{5+} and Ta^{5+} is higher than for Nb^{5+} and this increases the degree of covalency in the bonds formed. The covalent bonds have sp^3 hybridisation and this leads to further improvement in the piezoelectric properties of KNN–$LiTaO_3$–$LiSbO_3$ system.[18] The increment was initially attributed to the existence of a morphotropic phase boundary (MPB) at the proposed composition later reports show however, that the tetragonal to orthorhombic phase transition temperature is lowered to near room temperature and is therefore rather considered as a PPT.[19–21]

In this work we study the effect of adding MnO_2 on the densification, piezoelectric and dielectric properties of the KNN–$LiTaO_3$–$LiSbO_3$ system. Manganese was used because it has been reported to improve the densification of pure KNN.[16] Furthermore it is reported to suppress grain growth and helps to increase the electrical resistivity of the piezoceramic.

2. Experimental

The ceramics were synthesized through the mixed oxide route using the following powders; K_2CO_3 (99%), Na_2CO_3 (99%), Li_2CO_3 (99%), Sb_2O_3 (99.9%), Nb_2O_5 (99.9%), Ta_2O_5 (99%) (Chempur Feinchemikalien und Forschungs GmbH, Karlsruhe, Germany) and MnO_2 (99%) (Alfa Aesar, Karlsruhe, Germany).

Stoichiometric compositions of the powders were first weighed and dried at 220 °C for 4 h. They were then mixed and attrition milled for 4 h using ethanol as solvent and zirconia balls as the milling media. Calcination was carried out at 750 °C for 4 h after which the same attrition mill and calcination process were repeated.

The powders were pressed into discs of 12.5 mm diameter first using a uniaxial press at 170 MPa and later using a cold isostatic press at 500 MPa for 2 min. The pellets were sintered in air atmosphere at 1075 °C for 1 h.

The density of the samples was determined using the Archimedes method while pattern: 00-032-022 from ICDD was used as a reference structure to calculate the theoretical density. The crystalline structure of the sintered samples was examined using X-ray diffraction analysis with Cu Kα radiation (D8 Discover, Bruker AXS, Karlsruhe, Germany).

The samples were polished and thermally etched at 925 °C for 30 min. The microstructure was observed using a scanning electron microscope (LEO 1530 FESEM, Gemini/Zeiss, Oberkochen, Germany). Grain size measurements were carried out using the mean intercept length method from at least six different areas of the SEM image.

Silver paint acting as electrodes was applied on both surfaces of the sample. The temperature dependence of the dielectric properties of the ceramics was measured from 20 Hz to 1 MHz using an LCR meter (HP 4284A, Agilent Technologies, Inc., Palo Alto, USA) attached to a programmable furnace. The polarisation hysteresis curves were obtained using a Sawyer–Tower circuit while unipolar and bipolar strain hysteresis curves were obtained using an inductive transducer device. A complete hysteresis loop was performed in 3 min. The piezoelectric coefficient (d_{33}) was measured using a low signal displacement transducer connected to a lock-in amplifier which measures the amplitude. Approximately 65 V was applied on the samples while the amplitude value from the lock-in amplifier was used to calculate the charge coefficient.

3. Result and discussion

The density values for the KNN–$LiTaO_3$–$LiSbO_3$ ceramics doped with MnO_2 are as shown in Table 1. The theoretical density for the undoped sample is 4.79 g/cm^3 while the relative density was calculated to be 94.3%. Densification is improved up to 96.4% when an amount of 1 mol% MnO_2 is added. This is accompanied by a decrease in grain growth which is in agreement with other reports for pure KNN.[22,23] The SEM images of the thermally etched samples in both the undoped and doped form are shown in Fig. 1. For both compositions, cornered cubic grains were observed in the surfaces of the polished samples.

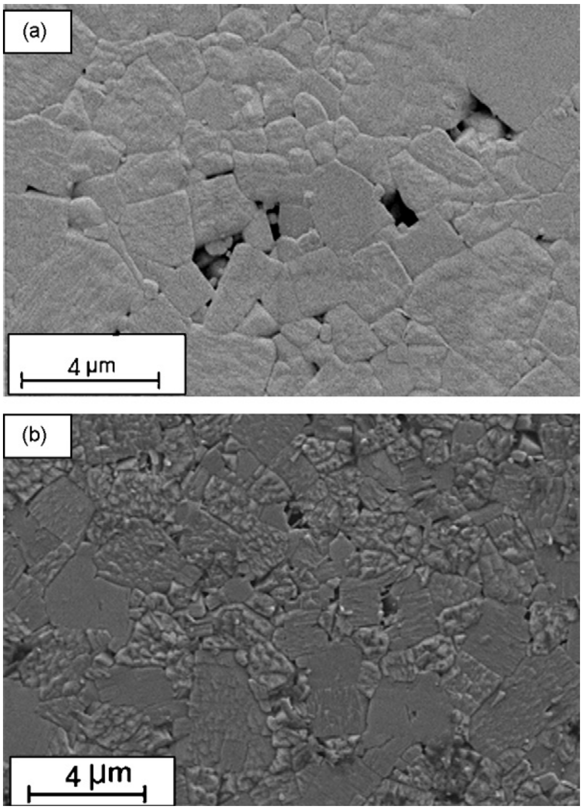

Fig. 1. SEM micrographs of the thermally etched KNN–$LiTaO_3$–$LiSbO_3$ samples that were sintered at 1075 °C for 1 h (a) undoped, (b) 0.5 mol% MnO_2.

The microstructures of the samples have some smooth and rough grains. This may be due to the different crystallographic planes, which behave differently during thermal etching. The higher energetic planes try to revert to the lower energetic planes and the result is a steeped/rough surface.

For the undoped sample (Fig. 1a), there is an inhomogeneous grain size distribution such that the grains have a bimodal grain size distribution with big grains being surrounded by small grains. The calculated average grain sizes are 7.3 ± 0.1 μm and 2.1 ± 0.1 μm for the big and small grains, respectively. Unevenly distributed relatively large pores can be seen at the grain boundaries. The shapes of the pores show that some of them may have been formed due to grain pull-out during polishing process than due to sintering.

In Fig. 1b, the sample doped with 0.5 mol% of MnO_2 shows a unimodal grain size distribution with an average grain size of approximately 2.1 ± 0.1 μm showing that the grain growth anomaly in the undoped sample is suppressed here because manganese is known to create oxygen vacancies thereby pinning the movement of the grain boundaries. Some researchers[24,25] have attributed this to the fact that Mn ions occupy both the A and B-sites of the perovskite structure. It is said that when PZT is doped with MnO_2, the site occupancy is determined by the amount of the dopant in the ceramic. Below 0.5 mol%, MnO_2 is believed to act as a donor and above that as an acceptor by occupying A-sites and B-sites, respectively. It is believed that this behaviour extends to the KNN solid solution.[23]

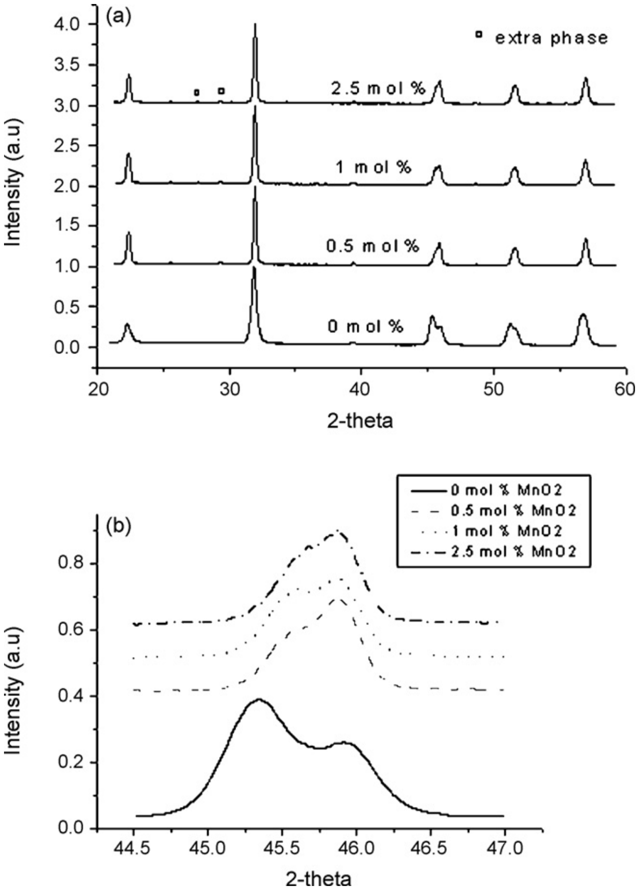

Fig. 2. XRD patterns of the polished surfaces of KNN–$LiTaO_3$–$LiSbO_3$ samples (a) doped with different amounts of MnO_2, (b) zoomed pattern from 44.5° to 47° showing the change from orthorhombic to tetragonal structure.

The XRD pattern of polished samples doped with different amounts of MnO_2 is shown in Fig. 2a. All the ceramics have a perovskite structure and in the undoped sample, the orthorhombic structure is the dominant phase at room temperature and changes to a predominantly tetragonal structure with increasing the amount of the dopant showing that the tetragonal-orthorhombic phase transition ($T_{T\text{–}O}$) is shifted to lower temperatures with addition of MnO_2.

Fig. 2b shows the change in the structure at 2θ angle of between 45° and 47° with increasing amount of MnO_2. The contribution of the different peak shapes to orthorhombic and tetragonal structures was shown by Wang and Li.[26]

Extra peaks (marked with a square) that appear with increasing amounts of the additive show that the solubility of MnO_2 in the KNN–$LiTaO_3$–$LiSbO_3$ solid solution is limited. The excess is believed to accumulate at the grain boundaries.[22] Peak search and match analysis was carried out using the ICDD, but due to their size these extra peaks could not be conclusively attributed to any structure.[27]

Fig. 3a shows the temperature dependent values of dielectric constant while Fig. 3b shows the loss tangent for the MnO_2 doped samples measured at 1 kHz. The addition of the Li^{1+}, Ta^{5+} and Sb^{5+} to pure KNN leads to the formation of a PPT reducing the first order phase transition to around room temperature.[26]

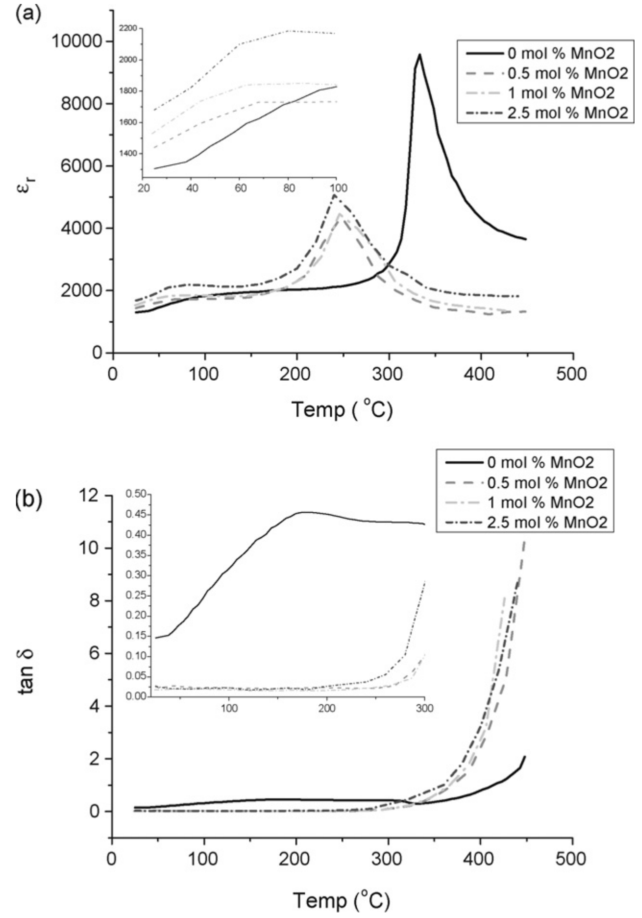

Fig. 3. (a) High temperature dielectric constant (ε_r) values for MnO_2 doped KNN–$LiTaO_3$–$LiSbO_3$ ceramics as a function of temperature. The inset shows ε_r values at lower temperatures on an enlarged scale. (b) High temperature dielectric loss (tan δ) values for MnO_2 doped KNN–$LiTaO_3$–$LiSbO_3$ ceramics as a function of temperature. The inset shows tan δ values at lower temperatures on an enlarged scale.

The KNN–$LiTaO_3$–$LiSbO_3$ system exhibits two phase transition peaks: The first is associated with $T_{T\text{–}O}$ near room temperature while the second is with the tetragonal to cubic phase transition at 333 °C and a dielectric peak of approximately 9500. These values are high when compared to the results by other researchers.[13] This could be a result of the difference in the sintering atmosphere used, powder processing methods and parameters used or even from the starting raw materials. Addition of MnO_2 reduces the T_c to about 249 °C which did not decrease much further with increased doping amount. Addition of dopants is known to change microstructures substantially and affect crystalline phase of samples.[18] The doped samples have rounded peaks which is an indication of a decrease in ferroelectricity. The dielectric loss values in Fig. 3b show that the addition of the dopants reduced the dielectric loss in the samples to approximately 2.5% at temperatures below 300 °C. The loss in the undoped sample is however higher than those obtained by other researchers.[18,28] For the manufacturing of devices like transformers that require very low dielectric loss values even at elevated temperatures, the doped composition could be explored as has been done in some reports.[29]

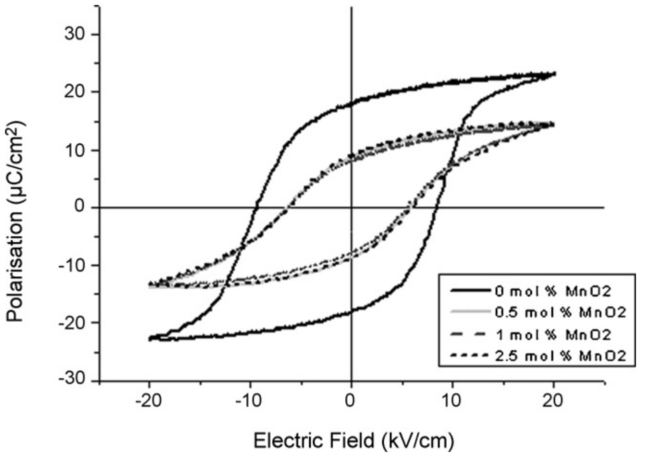

Fig. 4. Variation of P–E hysteresis loops for MnO_2 doped KNN–$LiTaO_3$–$LiSbO_3$ ceramics.

The polarisation hysteresis curves for the undoped and doped samples are shown in Fig. 4. The entire curves show saturation polarisation when an electric field ∼20 kV/cm is applied. The addition of manganese lowered the coercive field (E_c) and the remanent polarisation values. This is interesting because lower coercive fields are usually attributed to donor doped piezoceramics while lower remnant polarisations are commonly found in acceptor doped ceramics. Additionally the doped ceramics exhibit a lower area of the hysteresis loop and as a result hysteretic losses are lower too. However, there is no significant difference with increasing amount of dopant.

In Fig. 5, the strain hysteresis loops of the undoped and manganese doped ceramics are shown. All compositions had the typical butterfly shape which shows that they are ferroelectric. The doped ceramics all exhibited a smaller hysteretic behaviour than the undoped ceramic. This may be explained by the acceptor doping effect of the dopant on KNN–$LiTaO_3$–$LiSbO_3$ ceramics.

The highest value of the piezoelectric charge coefficient (d_{33}) for the samples as shown in Table 1 is from the undoped sample. The amount of MnO_2 added did not significantly change the d_{33} values. The reason for the reduction could be attributed to the fact

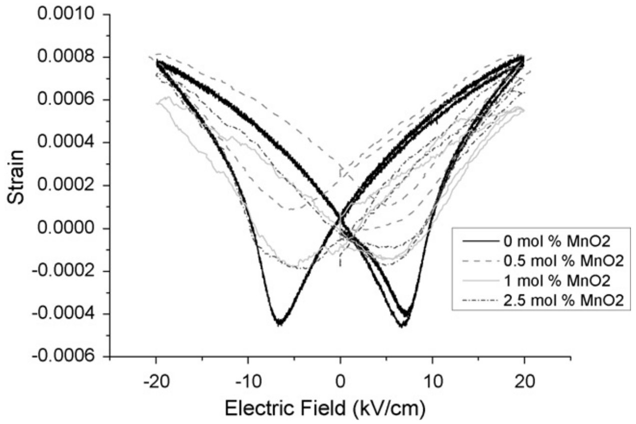

Fig. 5. Variation of strain-field hysteresis loops for MnO_2 doped KNN–$LiTaO_3$–$LiSbO_3$ ceramics.

that addition of the dopants led to a decrease in the distortion of the crystal structure as can be seen in the reduced peak splitting in Fig. 2.

4. Conclusion

Addition of MnO_2 to the KNN–$LiTaO_3$–$LiSbO_3$ improved the density of the sintered ceramics by inhibiting grain growth. The addition of MnO_2 induced a phase transformation from orthorhombic to the tetragonal structure at room temperature, a decrease in the T_c and a slight shift in the T_{T-O} phase transition. The dielectric loss values were reduced by doping with MnO_2 even at higher temperatures. Adding MnO_2 led to a reduction in the piezoelectric charge coefficient (d_{33}), the remanent polarisation, coercive field and strain hysteresis loops, respectively. Increasing amounts of dopants result in the formation of extra phases and do not significantly change the piezoelectric properties.

Acknowledgement

This work was supported by the scholarship granted by the European commission through the Erasmus Mundus programme for masters' degree studies in materials science.

References

1. Council Epat, Directive 2002/95/EC of the European parliament and of the council of January 2003 on the restriction of the use of hazardous substances in electrical and electronic equipment. *Eur. J.*, 2003, **37**, 19.
2. Toda, K., Ohtake, N., Kawakami, M., Tokuoka, S., Uematsu, K. and Sato, M., Characterisation of potassium niobate produced by self-assembled nanosheet from aqueous solution. *Jpn. J. Appl. Phys.*, 2002, **41**(11B), 7021–7024.
3. Hiruma, Y., Aoyagi, R., Nagata, H. and Takenaka, T., Ferroelectric and piezoelectric properties of $(B_{1/2}K_{1/2})TiO_3$ ceramics. *Jpn. J. Appl. Phys.*, 2005, **44**(7A), 5040–5044.
4. Takenaka, T., Sakata, K. and Toda, K., Piezoelectric properties of $(Bi_{1/2}Na_{1/2})TiO_3$-based ceramics. *Ferroelectrics*, 1990, **106**, 375–380.
5. Egerton, L. and Dillion, D. M., Piezoelectric and dielectric properties of ceramics in the system potassium–sodium niobate. *J. Am. Ceram. Soc.*, 1959, **42**, 438–442.
6. Jaeger, R. E. and Egerton, L., Hot pressing of potassium–sodium niobates. *J. Am. Ceram. Soc.*, 1962, **45**, 209–213.
7. Ahn, Z. S. and Schulze, W. A., Conventionally sintered $(Na_{0.5}\,K_{0.5})NbO_3$ with barium additions. *J. Am. Ceram. Soc.*, 1987, **70**, 18–21.
8. Guo, Y., Kakimoto K.-i. and Ohsato, H., Dielectric and piezoelectric properties of lead-free $(Na_{0.5}\,K_{0.5})NbO_3$–$SrTiO_3$ ceramics. *Solid State Commun.*, 2004, **129**, 279–284.
9. Kosec, M., Bobnar, V., Hrovat, M., Bernard, J., Malic, B. and Holc, J., New lead-free relaxors based on the $K_{0.5}\,Na_{0.5}NbO_3$–$SrTiO_3$ solid solution. *J. Mater. Res.*, 2004, **19**(6), 1849–1854.
10. Kakimoto K.-i., Akao, K., Guo, Y. and Ohsato, H., Raman scattering study of piezoelectric $(Na_{0.5}\,K_{0.5})NbO_3$–$LiNbO_3$ ceramics. *Jpn. J. Appl. Phys.*, 2005, **44**(9B), 7064–7067.
11. Hollenstein, E., Davis, M., Damjanovic, D. and Setter, N., Piezoelectric properties of Li and Ta modified $(K_{0.5}\,Na_{0.5})NbO_3$ ceramics. *Appl. Phys. Lett.*, 2005, **87**, 182905, pp. 1–3.
12. Zang, G.-Z., Wang, J.-F., Chen, H.-C., Su, W.-B., Wang, C.-M., Qi, P., Ming, B.-Q., Du, J. and Zheng, L.-M., Perovskite $(Na_{0.5}K_{0.5})_{1-x}(LiSb)_xNb_{1-x}O_3$ lead-free piezoceramics. *Appl. Phys. Lett.*, 2006, **88**, 212908, pp. 1–3.
13. Saito, Y., Takao, H., Tani, T., Nonoyama, T., Takatori, K., Homma, T., Nagaya, T. and Nakamura, M., Lead-free piezoceramics. *Nature*, 2004, **432**, 84–87.
14. Matsubara, M. and Kikuta, K. S. H., Piezoelectric properties of $(K_{0.5}Na_{0.5})(Nb_{1-x}Ta_x)O_3$–$K_{5.4}CuTa_{10}O_{29}$ ceramics. *J. Appl. Phys.*, 2005, **97**, 114105, pp. 1–7.
15. Chen, R. and Li, L., Sintering and electrical properties of lead-free $Na_{0.5}\,K_{0.5}NbO_3$ piezoelectric ceramics. *J. Am. Ceram. Soc.*, 2006, **89**(6), 2010–2015.
16. Ahn, C.-W., Song, H.-C., Nahm, S., Park, S.-H., Uchino, K., Priya, S., Lee, H.-G. and Nam-Kee, K., Effect of MnO_2 on the piezoelectric properties of $(1-x)(Na_{0.5}K_{0.5})NbO_{3-x}BaTiO_3$ ceramics. *Jpn. J. Appl. Phys.*, 2005, **44**, L1361–L1364.
17. Du, H., Liu, D., Tang, F., Zhu, D. and Wancheng, Z., Microstructure, piezoelectric, and ferroelectric properties of Bi_2O_3-added $(K_{0.5}Na_{0.5})NbO_3$ lead-free ceramics. *J. Am. Ceram. Soc.*, 2007, **90**, 2824–2829.
18. Hagh, N. M., Jadidian, B. and Safari, A., Property-processing relationship in lead-free (K, Na, Li) NbO_3-solid solution system. *J. Electroceram.*, 2007, **18**, 339–346.
19. Shrout, T. R., Eitel, R., Randall, C. A., Alberta, E. and Rehrig, P. W., New high temperature morphotropic phase boundary piezoelectric ceramics, applications of ferroelectrics, ISAF 2002. In *Proceedings of the 13th IEEE International Symposium on ferroelectrics*, 2002, pp. 277–280.
20. Shrout, T. R., Zhang, S. J., Eitel, R., Stringer, C. and Randall, C. A., High performance, high temperature perovskite piezoelectrics, applications of ferroelectrics, ISAF-04. In *14th IEEE International Symposium*, 2004, pp. 26–129.
21. Akdogan, E. K., Kerman, K., Abazari, M. and Safari, A., Origin of high piezoelectric activity in ferroelectric $(K_{0.44}Na_{0.52}Li_{0.04})(Nb_{0.84}Ta_{0.1}Sb_{0.06})O_3$ ceramics. *Appl. Phys. Lett.*, 2008, **92**, 112908, pp. 1–3.
22. Tashiro, S., Ishii, K. and Wada, T., Fabrication of $(Sr_xK_{0.5-x}Na_{0.5-x})NbO_3$ pizoelectric ceramics and effects of MnO addition on their piezoelectric properties. *Jpn. J. Appl. Phys.*, 2006, **45**(9B), 7449–7454.
23. Lin, D., Kwok, K. W., Tian, H., Wong, H. and Chan, L-w., Phase transitions and electrical properties of $(Na_{1-x}K_x)(Nb_{1-y}Sb_y)O_3$ lead-free piezoelectric ceramics with a MnO_2 sintering aid. *J. Am. Ceram. Soc.*, 2007, **90**, 1458–1462.
24. He L.-x. and Li, C.-e., Effects of addition of MnO on piezoelectric properties of lead zirconate titanate. *J. Mater. Sci.*, 2000, **35**, 2477–2480.
25. Klimov, V. V., Selikova, N. I. and Bronnikov, A. N., Effect of MnO_2, Bi_2O_3, and ZnO additions on the electrical properties of lead zirconate titanate piezoceramics. *Inorg. Mater.*, 2006, **42**(5), 573–577.
26. Wang, K. and Li, J.-F., Analysis of crystallographic evolution in $(Na,K)NbO_3$-based lead free piezoelectrics by X-ray diffraction. *Appl. Phys. Lett.*, 2007, **91**, 262902, pp. 1–3.
27. Ming, B.-Q., Wang, J.-F., Qi, P. and Zang, G.-Z., Piezoelectric properties of (Li,Sb,Ta) modified $(Na,K)NbO_3$ lead-free ceramics. *J. Appl. Phys.*, 2007, **101**, 054103, pp. 1–4.
28. Hagh, N. M., Ashbahian, E. and Safari, A., Lead-free piezoelectric ceramic transducer in the $K_{1/2}Na_{1/2}NbO_3$-solid solution system. *IEEE-UFFC Trans.*, 2008, **55**(1), 214–224.
29. Guo, M., Lam, K. H., Lin, D. M., Wang, S., Kwok, K. W., Chan, H. L. W. and Zhao, X. Z., A Rosen-type piezoelectric transformer employing lead-free $K_{0.5}Na_{0.5}NbO_3$ ceramics. *J. Mater. Sci.*, 2008, **43**, 709–714.